Characterization and modification of SrS based blue thin film electroluminescent phosphors

Wei-Min Li

Laboratory of Inorganic Chemistry
Department of Chemistry
University of Helsinki
Finland

Academic Dissertation

To be presented, with the permission of the Faculty of Science of the University of Helsinki, for public criticism in Auditorium A110 of the Department of Chemistry on January 14, 2000, at 12 noon.

ISBN 951-45-8991-2 (PDF version)
Helsingin yliopiston verkkojulkaisut
Helsinki 2000

Supervisor

Prof. Markku Leskelä
Laboratory of Inorganic Chemistry
Department of Chemistry
University of Helsinki
Finland

Reviewers

Dr. Hannu Kattelus
VTT Electronics
Finland

Dr. Juha Viljanen
Planar Systems Inc.
Finland

Opponent

Dr. Kristiaan Neyts
Electronic & Information Systems Department
University of Ghent
Belgium

Abstract

State-of-the-art SrS based blue thin film electroluminescent (TFEL) phosphors, namely, SrS:Ce, SrS:Cu, and SrS:Ag,Cu,Ga, were characterized by combined ion beam analysis techniques and photoluminescence (PL) and electroluminescence (EL) measurements. A selection of different elements were ion implanted into SrS:Ce and SrS:Cu thin films and their effects on the luminescence properties of the phosphor materials were examined.

Impurities in thin films of SrS:Ce made by Atomic Layer Epitaxy (ALE) and SrS:Ce,Mn,Cl made by reactive evaporation were analyzed by various ion beam techniques, viz. Rutherford backscattering spectroscopy, elastic recoil detection analysis (ERDA), time-of-flight (TOF)-ERDA, nuclear resonance broadening, proton induced x-ray emission, particle induced γ-ray emission, and deuteron induced reactions. All samples were of high purity, with Sr/S or (Sr+Mn)/S ratio close to unity. The major impurities in the thin film bulk were H, C, and O. In ALE SrS:Ce, good EL performance correlated with an overall low impurity content, in particular low C content. In intentionally codoped SrS:Ce,Na samples, Na was found to concentrate at the phosphor–insulator interface. The EL performances of the corresponding TFEL devices were poor. For the reactively evaporated SrS:Ce,Mn,Cl samples, the EL performances were better than the ALE SrS:Ce devices despite their higher levels of H, C, and O impurities.

Ion implantation of ALE SrS:Ce thin films with Na, K, Ag, P, Ga, F, and Cl showed that positive ions may be more favorable as codopants than negative ions. Implantation of F resulted in about 10 nm blue shift of the emission, but annealing above 500 °C quenched the PL intensity. K implantation enhanced the PL intensity by a factor of two when annealed at 800 °C, and even greater enhancement was achieved with Ag implantation under the same annealing conditions. Blue shift of about 10 nm was also present in these samples as a result of high temperature annealing. Implanted SrS:Ce,Ag exhibited the best decay value (S_N=22 ns) ever reported for ALE SrS:Ce thin films and the EL results are encouraging. Implantation of Cl and Na did not improve the PL of SrS:Ce thin films, while P and Ga quenched the luminescence.

Negative ions seem to be more favorable as codopants for SrS:Cu, perhaps as a result of the presence of S vacancies. Implantation of F, Cl, and O enhanced the PL emission. SrS:Cu,Cl also exhibited a pronounced blue shift of the green emission band. Implantation of B also improved the emission intensity, but the oxidation state of B is yet undetermined. Implantation of Ag, Al, and Ga did not improve the PL intensity. Nevertheless, a few SrS:Cu,Ag films showed the blue band due to Ag emission.

It was verified that both blue and green emission may be observed in SrS:Cu at room temperature. The color gamut is determined by the intensity ratio of two emission bands located at 460 (H band) and 520 nm (L band). The L band is attributed to the emission of isolated Cu^+ ion substitutes octahedral coordinated Sr but at off–center position and the H band to Cu^+ at a different site symmetry. Luminescence of SrS:Cu is likely to follow a three–level mechanism as characterized by the increased decay time with decreasing temperature. The completely green luminescence of SrS:Cu with a single band located above 520 nm possibly originates from Cu pairs and aggregated Cu centers. The blue luminescence of SrS:Ag,Cu,Ga may be related to Ag^+–Ag^+ pairs or Ag^+–(Cu^+) associated centers, or both.

List of publications

This thesis consists of the following original articles that have been published or accepted in international journals. The papers are referred to in the text by the accompanying Roman numerals.

I. M. Leskelä, W.-M. Li, and M. Ritala, Materials in thin film electroluminescent devices. *Semiconductors and Semimetals, Electroluminescence II* Vol. **65** (ed. G. Müller), Academic Press, 1999, pp. 107-182.

II. W.-M. Li and M. Leskelä, Luminescence of Ce^{3+} in alkaline earth chloride lattices, *Mater. Lett*. **28** (1996) 491-498.

III. W.-M. Li, M. Ritala, M. Leskelä, R. Lappalainen, J. Jokinen, E. Soininen, B. Hüttle, E. Nykänen, and L. Niinistö, Elemental characterization of electroluminescent SrS:Ce thin films, *J. Appl. Phys*. **84** (1998) 1029-1035.

IV. R. Lappalainen, J. Jokinen, W.-M. Li, M. Ritala, M. Leskelä, and E. Soininen, Complementary analysis of ALE-grown SrS based thin film electroluminescent structures with ion beam methods, *Nucl. Instr. Meth. Phy. Res. B* **132** (1997) 685-696.

V. W.-M. Li, M. Ritala, M. Leskelä, R. Lappalainen, M. Karjalainen, E. Soininen, C. Barthou, P. Benalloul, J. Benoit, E. Nykänen, and L. Niinistö, Ion implantation of SrS:Ce thin films, *J. Soc. Information Display.*, (1998) in press.

VI. W.-M. Li, M. Ritala, M. Leskelä, R. Lappalainen, E. Soininen, L. Niinistö, C. Barthou, P. Benalloul, and J. Benoit, Improved blue luminescence in Ag-codoped SrS:Ce thin films made by atomic layer epitaxy and ion implantation, *Appl. Phys. Lett*. **74** (1999) 2298-2300.

VII. W.-M. Li, M. Ritala, M. Leskelä, R. Lappalainen, L. Niinistö, E. Soininen, S.-S. Sun, W. Tong, and C.J. Summers, Photo- and electroluminescence of SrS:Cu and SrS:Ag,Cu,Ga thin films, *J. Appl. Phys*., **86** (1999) 5017-5025.

Symbols and abbreviations

τ	Decay time
η	Efficiency
λ	Wavelength
(thd)	(2,2,6,6-Tetramethyl-3,5-heptanedione)
ac	Alternating current
ALE, ALD	Atomic layer epitaxy, atomic layer deposition
CIE	Commission Internationale de l'Eclairage
CRT	Cathode ray tube
CVD, MOCVD	Chemical vapor deposition, Metal-organic CVD
dc	Direct current
EDS	Energy dispersive spectroscopy
EL	Electroluminescence
ITO	Indium tin oxide
L	Luminance
LCD	Liquid crystal display
MBE	Molecular beam epitaxy
NRB	Nuclear resonance broadening
PIGE	Particle induced gamma-ray emission
PIXE	Proton induced x-ray emission
PL	Photoluminescence
RBS, BS	Rutherford backscattering spectroscopy
S_N	Integrated decay value
TCO	Transparent conducting oxide
TEM	Transmission electron microscopy
TFEL	Thin film electroluminescence
TOF-ERDA	Time-of-flight elastic recoil detection analysis

Contents

1. Introduction

Electroluminescence (EL) is a non-thermal light emitting process resulting from the application of an electric field to a solid material. A simple alternating current thin-film electroluminescent (ACTFEL) device consists of a metal–insulator–semiconductor–insulator–metal (MISIM) structure deposited on a substrate, usually being glass. (Fig. 1)

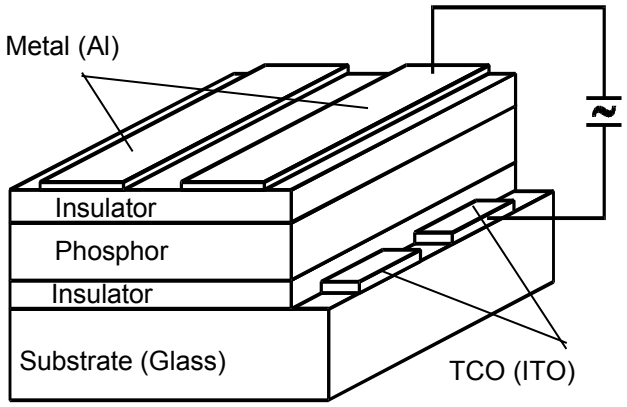

Fig. 1. Illustration of a monochrome ACTFEL display. Transparent conducting oxide (TCO) electrodes such as indium tin oxide (ITO) are used together with a glass substrate that allows the information to be viewed.

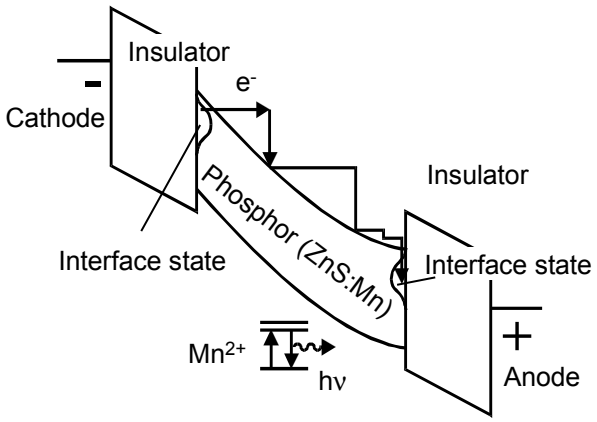

Fig. 2. Energy-band diagram of a ZnS:Mn based EL divice.

In a typical ZnS:Mn based EL device, high electric field (on the order of 10^8 V/m) causes tunnel injection of electrons from the interface states at one of the phosphor/insulating layer interfaces into the phosphor conduction band. The injected electrons are accelerated in

the high field, where they gain enough kinetic energy to impact excite the luminescence center of the phosphor. Light emission is realized at the luminescence center via the relaxation of electrons from the excited state to the ground state. The high-energy electrons that pass through the phosphor layer are trapped at the other phosphor/insulator interface causing an internal polarization. An energy-band diagram of the EL mechanism is illustrated in Fig. 2. The same process takes place in the opposite direction of the EL device when the polarity of the applied ac field is reversed.

Electroluminescence was first demonstrated by Destriau in 1936,[1] who put copper doped zinc sulfide crystals into castor oil and applied alternating current to produce light. The voltage he used was as high as 15 kV but the luminance was extremely poor. Nevertheless, the Destriau cell triggered great interest in EL as the "source de lumière du futur". The early stage of EL development during the 50s and 60s was mainly concentrated with dc and ac powder cells. It ended without much success, however, owing to the poor performance and reliability of the devices. The situation of today's powder EL has not changed much though improvements have been made in efficiency and stability. A few applications based on powder EL, such as backlight for LCDs, have proved attractive.

The advent of TFEL was marked by a paper by Inoguchi et al. in 1974,[2] reporting a TFEL device of ZnS:Mn sandwiched between two insulators which showed surprisingly high luminance and extremely long operating life under an ac electric field. During the past 25 years, ACTFEL has progressed from the commercialization of monochromic flat panel displays in the early 80s to the development of multi-color and full-color displays in the 90s. Current TFEL displays provide high brightness and contrast, wide viewing angle, fast response time, ruggedness to shock and vibration, wide temperature range, and long operating life. These features meet the requirements for demanding applications such as industrial process control and instrumentation, medical equipment, civil and military avionics, and transportation. The rapid progress has turned the fiction of "light source of the future" into reality.

Lack of true full-color TFEL materials, nevertheless, has prevented EL displays from penetrating further into an already highly competitive display market. While efficient green and red light can be achieved by filtering the yellow emission from ZnS:Mn, the biggest and

the most challenging problem is to find a satisfactory blue phosphor. Strontium sulfide based blue phosphors, such as SrS:Ce, SrS:Cu, and SrS:Ag,Cu, are the most promising candidates so far.

Bluish-green emitting SrS:Ce was already studied as a blue TFEL phosphor in 1984,[3] but the blue portion in its emission spectrum has been too small to meet the requirements for a full-color TFEL display. Significant efforts have been devoted to improving its EL performance. One frequently studied method is to modify the SrS:Ce phosphor by adding codopants so that either emission intensity can be enhanced or the spectrum can be shifted towards blue. Only recently, improved blue emission and excellent EL performances have been obtained with codoped SrS:Ce,Ag,Mn,Cl (CIE_x=0.26, CIE_y=0.47, L_{50}=142 cd/m^2, η=2 lm/W, 60 Hz).[4] Meanwhile, newly developed SrS:Cu shows a good blue-color gamut (CIE_x=0.15, CIE_y=0.23);[5] in particular, SrS:Ag,Cu has true blue color (CIE_x=0.17, CIE_y=0.13) that almost matches the hue of the CRT blue phosphor.[6] The EL performances of SrS:Cu and SrS:Ag,Cu are satisfactory ($L_{40}\approx$34 cd/m^2, $\eta\approx$0.24 lm/W, 60 Hz).[7] Nevertheless, the luminescence mechanisms of these new phosphors are poorly understood.

The aim of the study was to better understand and to improve state-of-the-art SrS based blue TFEL materials, namely SrS:Ce, SrS:Cu, and SrS:Ag,Cu phosphors. An extensive review of all materials used in TFEL displays is included in the list of publications [I]. Therefore, the present summary only briefly describes the concept and current status of TFEL that is related to this work. The experiments that were carried out focused on the effects of various impurity ions on the luminescence of the SrS based phosphors. Both intrinsic impurities in the phosphors and intentionally added impurities (codopants) were studied by combined ion beam analysis techniques, ion beam implantation and PL (photoluminescence) and EL measurements. Possible luminescence mechanisms for the new SrS:Cu and SrS:Ag,Cu blue phosphors are proposed.

2. Experimental

The experiments are summarized into three major parts. First, impurity contents that may affect the EL properties of currently the best SrS:Ce based thin films prepared by Atomic Layer Epitaxy (ALE) and reactive evaporation were investigated by combined ion beam analysis techniques. Second, ALE deposited SrS, SrS:Ce and SrS:Cu thin films were modified by implantation of selected ions and their luminescence properties were studied. Related to this, to understand the role of chlorine in the luminescence of SrS:Ce, study was made of the luminescence of cerium in powder alkaline earth chloride hosts. Third, PL and EL of the recently developed SrS:Cu and SrS:Ag,Cu materials were examined.

2.1. Sample preparation

For the experiments, SrS based thin films of different structure were prepared by several deposition techniques. Typically, SrS phosphor thin films having a thickness of about 500 nm were deposited on glass substrates coated with ITO transparent electrodes underneath an Al_2O_3 insulating layer. Occasionally, silicon wafers were used as substrates. For ion beam analyses of impurity contents in the phosphor layer, the structures were covered *in situ* or *ex situ* with 10, 35, or 100–200 nm of a protecting Al_2O_3 layer. Some samples also had an *in situ* deposited ZnS protective layer (about 100 nm). For ion implantation studies, 500-nm-thick ALE SrS films with Ce doped in the top 100-nm layer were used, as well as fully Ce doped films. An *in situ* 10-nm Al_2O_3 layer was deposited on top of the SrS layer to protect the phosphor from moisture and contamination. To allow EL measurements of the implanted samples, a further 200 nm Al_2O_3 top insulation layer was deposited after a heat treatment of the samples. In the case of the SrS:Cu and SrS:Ag,Cu samples used for ion implantation and/or luminescence studies, the as deposited phosphor films were first subjected to heat treatment without a protecting layer, and the top Al_2O_3 insulating layer was deposited afterwards to complete the EL structures.

The following text briefly describes the phosphor deposition techniques employed in this study.

ALE, also known as ALD (atomic layer deposition) and AL-CVD (chemical vapor deposition), and under some other names, is one of the major deposition techniques for producing high quality commercial TFEL displays. The technique is based on sequential surface reactions of different chemical precursors in a self-limiting manner, and the thin film is grown in layer-by-layer fashion with a precise thickness and high conformality.[8] Crystalline SrS:Ce thin films are deposited by using $Sr(thd)_2$, $Ce(thd)_4$ or $Ce(cp)_3$, and H_2S precursors at a substrate temperature of about 380 °C.[9,10] (thd=2,2,6,6-tetramethyl-3,5-heptanedione, cp=cyclo-pentadenyl) Except for the electrodes, the whole EL structure is prepared in vacuum with a single pump-down. After a necessary thermal treatment at about 515 °C, excellent EL performances with L_{40} of >90 cd/m^2 at 60 Hz driving condition can be routinely obtained. The ALE technique is also able to produce SrS:Cu thin films with both blue and green EL with $Cu(thd)_2$ as Cu precursor. Suitable Ag precursors for ALE are unavailable, however, and codoping of Ag into SrS:Ce and SrS:Cu by ALE has yet to be realized.

In reactive evaporation, SrS:Ce,Cl thin films are deposited in ultra-high vacuum at substrate temperature above 600 °C with elemental Sr, S, and powder $CeCl_3$ used as source materials. High luminance and efficiency can be achieved by the addition of elemental Mn.[11] The advantages of reactive evaporation technique are the flexibility to choose the reactants and to control the stoichiometry of the thin film. EL performances have been further improved by the addition of ZnS as the result of filling the S vacancies.[12] The as deposited films are highly crystallized and no further heat treatment is necessary. However, preparation of an EL device requires deposition of a top insulating layer in a separate step. Recently, an even further enhancement of EL performance has been made by codoping with Ag. Reactive evaporated SrS:Ce,Ag,Mn,Cl reached L_{50} of 170 cd/m^2 at 60 Hz driving condition.[13] This is the highest luminance ever achieved for SrS:Ce based materials.

Sputtering is a frequently used thin film deposition technique. The use of single target source material and the high energy of sputtered atoms during the deposition process make it a feasible method for producing films with complex composition while maintaining good stoichiometry. The new SrS:Cu and SrS:Ag,Cu blue phosphors studied in this work were deposited by rf magnetron sputtering at substrate temperature 150–350 °C.[5,7] Owing to the intrinsic characteristics of the sputtering process, the crystallinity of the as deposited films is

poor, but it can be greatly improved by post deposition RTA at about 800 °C. The top insulating layer was deposited after the heat treatment.

Several SrS:Cu samples were also prepared by molecular beam epitaxy (MBE). The technique is well known to produce high quality thin films, but it has not been employed in TFEL device production owing to the high cost of the equipment. Similar to ALE and sputtered SrS:Cu films, MBE SrS:Cu films require post deposition annealing at 800 °C.[14]

2.2. Ion beam analysis techniques

Ion beam analyses are based on interactions between a bulk material and energetic ion beams produced by an accelerator. With a suitable instrument set-up, information on element content and a depth profile of the target sample can be obtained through methods of detection that are specific to individual elements. These methods include back scattering (BS), elastic-recoil-detection analysis (ERDA), particle-induced x- or γ-ray emission (PIXE, PIGE), nuclear reaction analysis (NRA), and nuclear resonance broadening (NRB). Most of the methods used in this study employed a 2.4 MV Van de Graaff accelerator which is able to generate $^{1}H^{+}$, $^{2}H^{+}$, and $^{4}He^{+}$ ion beams. For the Time-of-Flight (TOF)-ERDA, ion beams of $^{197}Au^{7+}$ or $^{127}I^{6+}$ were obtained from a 5 MV EGP-10-II tandem accelerator.

Table I. Comparison of ion beam techniques used for SrS:Ce thin film impurity analysis.

Method	Element range (Z)	Detection limit	Concentration distribution	Purposes for this work
RBS	>20	0.1 at.%	Accurate	Ce, Mn concentration; Stoichiometry; Depth profiling; Main component analysis
PIXE	>20	1-100 ppm	None	General impurity analysis
PIGE	All (<30)*	1-100 ppm	None	Analysis of light elements
ERDA	All (<20)*	0.05 at.%	Moderate	H detection, profiling
TOF-ERDA	All (<20)*	0.01-0.1 at.%	Moderate	Detections of C, O, and Na
NRB	<20	1-100 ppm	Moderate	Detection of light elements, profiling

* The numbers in parentheses indicate the element range available for study in this work.

The advantages of ion beam methods in thin film analysis are as follows: capable of detecting most of the elements down to hydrogen, quantitative, capable of depth profiling in a

range of a few nanometers to a few micrometers, and non-destructive nature. Thin film characterization is by no means an easy task, however, because each ion beam method has its own limitations and the composition and structure of thin films are often complicated. The diversity and complexity of trace impurities in thin films impose an even greater challenge for quantitative analysis. Fortunately, combined ion beam techniques are able to provide at least qualitative information. With effort, the impurity contents in a thin film can be detected with reasonable precision. Table I lists several ion beam techniques used for the impurity analysis of SrS:Ce based thin films, together with their capabilities in element range, detection limit and depth profiling, and their application in this work.

2.3. Ion beam modification

Ion implantation is an important technique widely used in the semiconductor industry. The simple process and the capability to implant almost any element in a controlled quantity also make it a very attractive tool for TFEL material studies. With the aid of ion beam analysis and PL and EL studies, the influences of different impurities on the luminescence properties and the mobility and concentration of dopants and codopants can be rapidly examined. In this case, the possibility to implant one type of ion at a time is advantageous as compared with codoping using chemical compounds, where the counter-ions are also codoped and it is difficult to know which ions are responsible for the observed effects. Furthermore, EL devices can be made from ion beam modified thin films.[15]

In this work, ion implantation of various elements into ALE grown SrS, SrS:Ce, and SrS:Cu thin films was carried out using an isotope separator with a maximum energy of 120 kV. The energies for each element were adjusted to obtain an implantation depth of about 100 nm. The wide range of the implantation doses correspond to average concentrations of 0.003–1.0 at.%. The dopant concentrations in normal EL devices usually are in the range of 0.1–0.5 at.%. To avoid complication, problems such as implantation profile, implantation-caused non-stoichiometry, and the effect of oxidation states of non-metal elements were not taken into consideration. Since implantation causes lattice damage to the phosphor, annealings at 500–800 °C in N_2 atmosphere for various periods (typically 2 hours) were performed for all implanted films.

2.4. PL and EL measurements

Photoluminescence measurement is one of the major methods employed for study of the luminescence properties of SrS based blue phosphors. Not only does the PL emission closely resembles the EL, but more importantly, PL excitation, decay and time resolved spectra studies are very helpful for understanding the luminescence mechanism of the phosphor. Many luminescence properties can be further explored with use of the low temperature facility.

Ultimately, luminance, efficiency, and CIE color coordinates of the films must be characterized through EL measurements. In this work, EL spectra and L-V curves were studied using an ac power supply operating at 60 Hz driving conditions.

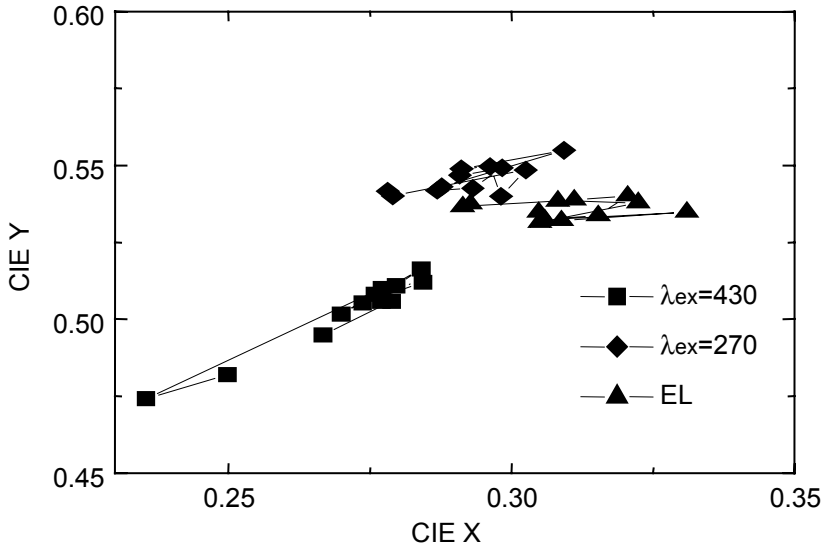

Fig. 3. PL and EL CIE color coordinates of a set of ALE SrS:Ce TFEL devices obtained with different excitation methods.

Quantitative comparison of the PL and EL properties of phosphor thin films is not always straightforward, however. A study on CIE coordinates of a set of SrS:Ce samples showed that the results do not correlate with each other when they are excited at Ce center (430 nm, PL), via host (270 nm, PL), or by EL excitation. (Fig. 3) Another frequently

encountered problem is the change of the emission spectrum due to optical interference within the thin film stack that consists of several layers having different refractive indices and a reflecting substrate or electrodes.[16] The interference is particularly strong when the substrate is Si or, in the case of EL measurement, the back electrodes are metallic. PL and EL properties from different samples may be compared, therefore, only if the thin film stacks are of identical structure and thickness, and have the same measurement geometry, even though the interference effects cannot be avoided by this way. To eliminate interference experimentally, one has to be able to integrate the light from the whole emission sphere. Yet another problem is the optical scattering originating from an opaque film, which may increase the measured PL and EL intensity. Also other factors should be taken into consideration, such as the phosphor film thickness and the amount of transferred charge in EL characterization (ΔQ, defined as total charge per unit area being transported across the phosphor layer between the two polarities). To compare the luminance and efficiency of ALE SrS:Ce and reactively evaporated SrS:Ce,Mn,Cl, the transferred charge is specified to 1 $\mu C/cm^2$.

3. Impurities in SrS:Ce based thin films

In principle, ion beam techniques are capable of detecting most of the elements in the periodic table [IV]. Even though the initial purpose of the analyses carried out in this work was to quantify all impurities in SrS:Ce based thin films, it was neither possible nor necessary to list every element in precision. A manageable solution was to isolate the problem from the complicated reality, therefore, to investigate only those impurities that are particularly interested in [III].

Impurity contents were compared for ALE SrS:Ce and reactively evaporated SrS:Ce,Mn,Cl thin films. In general, all samples studied were of high purity. The most noticeable impurities found were H, C, and O, and occasionally, weak signals corresponding to Ti, Cu, Mn, and Zn were detected. Figure 4 illustrates a case of Zn contamination in a reactive evaporated SrS:Ce/Si sample that was deposited after evaporating ZnS in the same chamber.

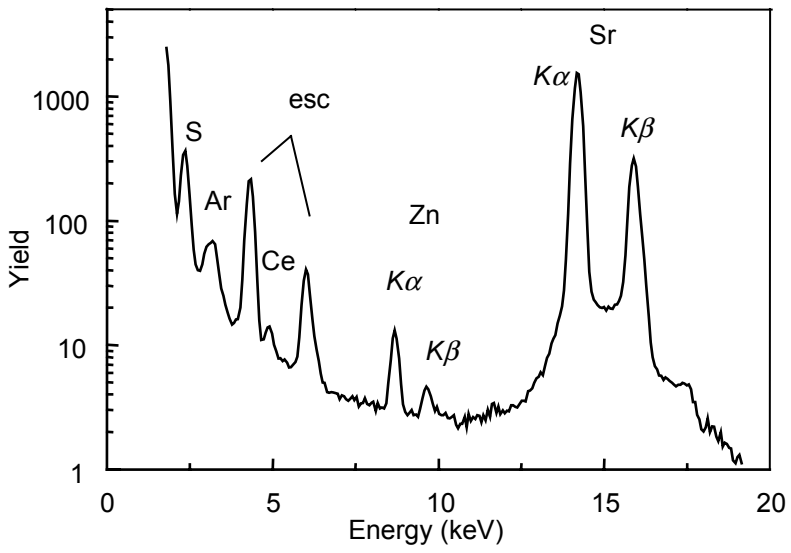

Fig. 4. PIXE spectrum of a SrS:Ce,Mn,Cl/Si sample prepared after deposition of ZnS in the same equipment. Signals from Zn are clearly visible.

The concentrations of H, C, and O impurities in various SrS:Ce based films made by ALE and reactive evaporation are summarized in Table II. The EL performances of TFEL devices made from the same batches as those used for analysis are listed for comparison.

Table II. Ion beam analysis of H, C, and O concentrations (at.%) in various ALE SrS:Ce and reactively evaporated SrS:Ce,Mn,Cl samples, and a comparison of their EL performances.

Preparation technique	Thin film structure	H (>0.1)	C (>0.03)	O (>0.06)	EL performances (1 μC/cm^2, 60 Hz)
ALE	35 nm Al_2O_3/SrS:Ce/ATO/Si(Glass)	0.2-0.7	<0.2	0.2-0.9	L_{25}= 42 cd/m^2,
	140 nm ZnS/SrS:Ce/Si	0.31	~0.11	0.08	η=1.2 lm /W
	140 nm ZnS/SrS/Si	<0.26	~0.05	0.05-0.09	
Reactive Evaporation	30 nm Al_2O_3/SrS:Ce,Mn,Cl/Si	1.3-1.8	0.2-0.7	0.5-1.8	L_{25}=75 cd/m^2,
	100 nm ZnS/SrS:$CeCl_3$/Si (in SrS)	0.6-1.0	0.2-0.7	0.8-1.3	η=1.6 lm /W
	100 nm ZnS/SrS:$CeCl_3$/Si (in ZnS)	-	0.04	0.05	

In ALE SrS:Ce covered *in situ* with Al_2O_3, the H and C concentrations are of the same magnitude as the concentration of Ce dopant (0.1–0.4 at.%) while the O concentration is slightly higher (0.2–0.9 at.%). It is known that the top Al_2O_3 layer introduces non-negligible interference signal for the oxygen measurement by TOF-ERDA. The oxygen content was significantly reduced (<0.1 at.%) when Al_2O_3 was replaced with ZnS as top layer. Comparison of the Ce doped and undoped ZnS/SrS films shows that each doped Ce atom brings with it less than one C and H atom. The ALE deposition process using $Sr(thd)_2$, $Ce(thd)_4$, and H_2S as precursors therefore produces SrS and SrS:Ce films with rather high purity.

Study on a set of ALE SrS:Ce based samples having a large variety of EL performances showed that higher concentrations of H, C, and O impurity reduce the EL luminance. Furthermore, a carbon profile across the substrate was observed in several ALE SrS:Ce samples, and examination of the corresponding EL devices showed that EL brightness increases with the decrease in carbon content along the flow direction of the reactants. Most likely, the thd ligands of the precursors undergo slight decomposition at the deposition temperature employed.

Another important finding was the relationship between sodium content and the EL performance. Sodium is used as codopant in SrS:Ce powder because of the charge mismatch of trivalent Ce with the host.[17] Codoping improves the Ce incorporation and accordingly also the PL properties. In the case of ALE SrS:Ce, however, codoping with Na has not made significant improvement in EL.[18] On the other hand, an early study showed that the Na contamination in ALE SrS:Ce thin films may occur when soda lime glass is used as

substrate.[19] Analysis of Na content was performed on a set of ALE SrS:Ce and SrS:Ce,Na films with different EL luminance. In Fig. 5, Na concentrations in SrS bulk and at the interface between the SrS and upper insulator were plotted against the EL luminances of the corresponding EL devices. As can be seen, Na contents were about the same in the SrS:Ce bulk (0.1–0.3 at.%) and in the SrS:Ce,Na bulk (0.2–0.4 at.%). These values are close to the detection limit of TOF-ERDA (0.1 at.%) and they are quite comparable to each other even though the EL performances of the samples vary a great deal. On the other hand, high Na content at the interface in these samples clearly indicates a weakening of the EL performance of SrS:Ce and SrS:Ce,Na thin films.

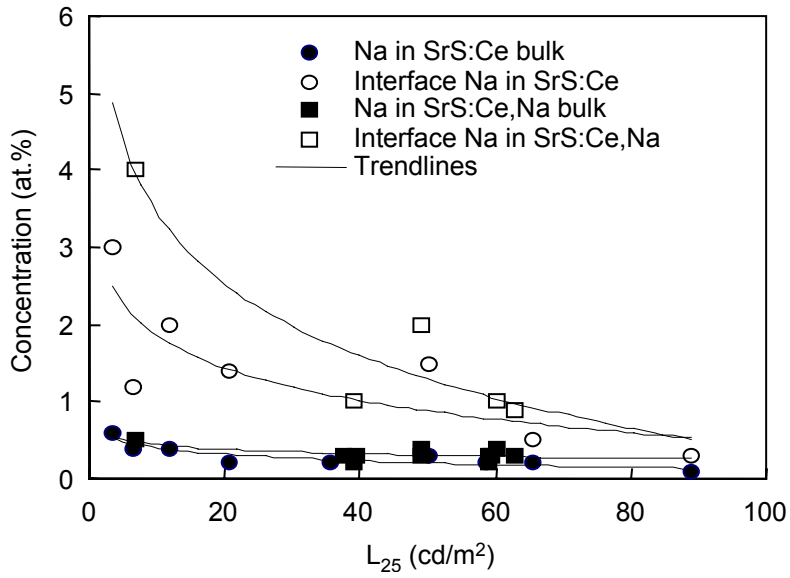

Fig. 5. Na concentration of ALE SrS:Ce and SrS:Ce,Na thin films vs the EL luminance of the corresponding EL device.

Compared with ALE SrS:Ce, higher contents of H, C, and O impurities were found in all reactively evaporated SrS:Ce,Mn,Cl films, suggesting that the H, C, and O impurities originate from the deposition process itself. (Table II) Possible contamination from air and moisture can not be completely ruled out, however, since Al_2O_3 layer is deposited *ex situ* after the SrS film has been exposed to air. Also the *in situ* deposited ZnS film is known to be highly polycrystalline and probably does not cat as a good passivation layer. Nevertheless, the reactively evaporated SrS:Ce,Mn,Cl samples did show better EL performances than the ALE SrS:Ce samples despite their higher impurity contents.

In relating the impurity contents to the EL properties of SrS:Ce thin films, however, one should be aware of the capability of and the information provided by the ion beam analysis techniques. Besides the stoichiometry of the phosphor bulk and its impurity contents, factors such as codopants, defects, crystallinity, and film morphology should be taken into consideration.

One limitation of the ion beam techniques is that they are unable to provide information on the location of the impurities in the polycrystalline films. The fact that reactively evaporated SrS:Ce,Mn,Cl gave better EL performances than ALE SrS:Ce samples, despite higher H, C, and O contents, hinted that impurities may influence the EL performance differently at different locations, for example in the crystal structure or at grain boundaries. There is no report on probing the local impurities in an EL phosphor. Apparently, this issue is also important for understanding the origin of space charges, which are crucial for EL performance. Besides the various vacancies, space charges have also often been associated with impurities, in both phosphor bulk and at phosphor/insulator interfaces. In this respect, alternative techniques such as transmission electron microscopy (TEM) combined with energy dispersive spectroscopy (EDS) may be considered. A TEM-EDS study on the SrS:Ce,Mn,Cl sample did show a higher concentration of Cl at the grain boundary than inside the grain.[20] The drawback of TEM-EDS is that the elements of low atomic number ($Z < 11$) cannot be detected.

Though combined ion beam techniques are capable of detecting the impurities at ppm levels, the depth profiling of low concentrations of impurities such as H, C, and O is difficult due to the low signal to noise ratio and strong signal disturbance from the top Al_2O_3 layer and surface contamination. A more consummate analyses may certainly be achieved by incorporate other analytical tools with ion beam techniques.[21] Nevertheless, routine ion beam analysis of particularly interesting impurities in the SrS:Ce thin films provided accurate enough information for the purpose of this study.

4. Ion beam modification of ALE SrS:Ce and SrS:Cu thin films

A variety of elements were implanted into ALE SrS, SrS:Ce, and SrS:Cu thin films in order to study their influence on the luminescence properties and to find possible dopants and codopants for improving SrS based blue EL phosphors. After necessary annealing, the luminescence of the ion beam modified samples was studied.

4.1 Implantation of SrS:Ce

The selection of elements for implanting in SrS:Ce was based on their anticipated function in the phosphor [V]. For example, Na, K, P, and newly discovered Ag may be substitutional cations, while F and Cl are interstitial anions. These ions are expected to compensate the charge mismatch, influence the crystal field, or act as co-activators in the SrS:Ce matrix. Gallium, on the other hand, is known to be a flux agent that improves the crystallinity and thereby the luminescence.

Compared with the reference ALE SrS:Ce, implantation of F resulted in a clear emission blue shift without decrease in the PL intensity when annealing was at above 500 °C. The blue shift increased to a maximum of about 10 nm with increasing F concentration. However, excessive F doses (0.5 at.% F as compared to ~0.2 at.% Ce) and high temperature annealing (>700 °C) reduced the decay time (S_N value* of 9.5 ns compared to the reference ALE SrS:Ce, which usually has a value of > 12 ns) and quenched the luminescence. A NRB study showed that there was severe F loss upon annealing and only traces (< 100 ppm) remained in the SrS:Ce bulk after annealing at 900 °C. In contrast to SrS:Ce,F, no clear spectrum blue shift was observed with implantation of the isoelectronic Cl and the emission intensity of SrS:Ce,Cl was less than that of the reference samples.

$CeCl_3$ and CeF_3 are frequently used source materials in the deposition of SrS:Ce by evaporation methods and sputtering.[22-24] Codoping of F or Cl has also been attempted by

* The decays of most of the SrS:Ce thin films are non-exponential as compared to the powder, which has a single decay time of τ_0=27 ns. The areas under the normalized decay curves are integrated, therefore, to obtain the S_N

ALE.[25,26] It is possible that the cerium ions are not entirely in a pure sulfide matrix but at least partially in a halide environment. Studies on Ce-doped alkaline earth chlorides showed that the Ce luminescence lies in the UV region and these hosts are able to incorporate rather large amount of Ce dopant (more than 5 mol.%) without concentration quenching [II]. But the UV emission from $SrCl_2$-type environment has not been observed in, for example ALE SrS:Ce,Cl ($SiCl_4$ as precursor) or in reactively evaporated SrS:Ce,Cl. It is likely that F and Cl may incorporate as charge compensators in the host. Some early work has suggested that the optimum Ce to halide ratio may be close to one.[27,28] In reactively evaporated SrS:Ce,Mn,Cl, loss of Cl was observed when higher temperature was used during both film deposition and post annealing as compared to that at optimized deposition condition, and as a consequence, the EL decreased.[29]

A number of studies have shown that codoping with F results in either a more pronounced blue emission shift or better EL performance as compared to codoping with Cl.[22,30] The implantation results seem to support such findings. It may be that F^- is more electronegative than Cl^- ion and hence results in higher excited energy levels of the Ce^{3+} ion. Furthermore, since the ionic radius of Cl^- is comparable to that of S^{2-}, while the F^- ion is much smaller, it is possible that F^- would locate at interstitial sites, while Cl^- would prefer substitutional sites, and the influence of the two ions on the luminescence of SrS:Ce might then be different. Thirdly, the finding of only traces of implanted F in high temperature annealed SrS:Ce,F suggests that codoped F may also act as a flux agent for better crystallization. On the other hand, since CeF_3 is thermally rather stable, it is understandable that $CeCl_3$ may be a better choice for the evaporation process, despite its hygroscopic nature. $CeCl_3$ is used in reactive evaporated SrS:Ce,Mn,Cl, and the EL performances are good.[31]

Unlike the implanted SrS:Ce,F samples whose PL was quenched after annealing at 700 °C, implantation of K into SrS:Ce resulted in an improved PL after annealing at above 700 °C compared to the reference SrS:Ce. Almost two-fold enhancement of the luminescence was achieved with SrS:Ce,K having optimum K doses and after annealing at 800 °C. Decay time studies showed that the S_N values of most of the SrS:Ce,K samples were comparable to those of the reference sample. A further study was conducted by implanting the same amount of Ce

---

values for a more precise comparison of the decay properties. The S_N/τ_0 ratio gives the internal luminescence

and K ions into undoped SrS film with partially overlapping implantation areas. As shown in Fig. 6, the codoped SrS:Ce,K not only had higher PL intensity than the singly doped SrS:Ce, but quenching of the samples did not occur in SrS:Ce,K at high annealing temperature and dopant concentration.

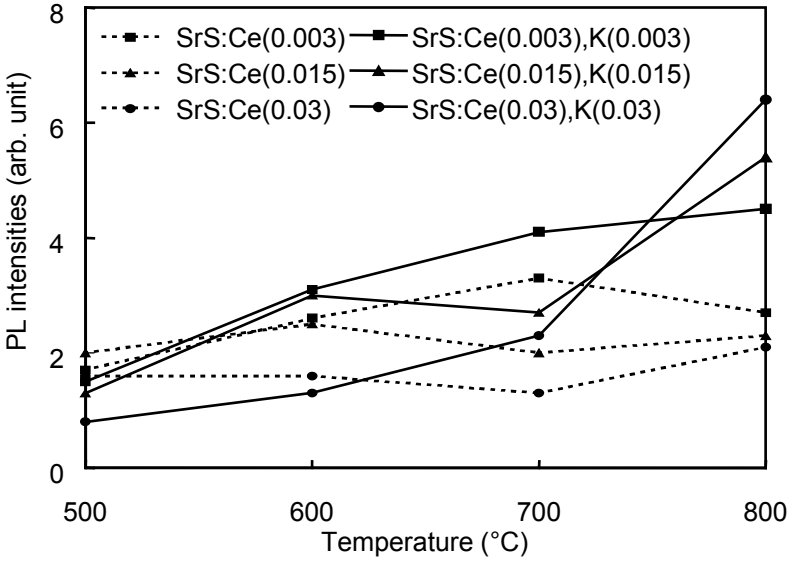

Fig. 6. Dependence of PL intensity on the annealing temperature of Ce,K co-implanted SrS with various Ce and K concentration. The solid lines represent SrS:Ce,K and the dotted lines singly implanted SrS:Ce.

Sodium is used as a charge compensator in SrS:Ce,Na powders.[17] However, the beneficial effects of K implantation were not observed in Na implanted SrS:Ce. It may be relevant that the ionic radius of Na^+ (1.02 Å) is smaller than that of Sr^{2+} (1.18 Å) and K^+ (1.38 Å). In the case of Ce doped alkaline earth chlorides [II], even though codoping of Na^+ or K^+ ions enhances the luminescence of both $CaCl_2$:Ce and $SrCl_2$:Ce, but $CaCl_2$:Ce,Na shows more intense luminescence than $CaCl_2$:Ce,K, while $SrCl_2$:Ce,Na shows weaker luminescence than $SrCl_2$:Ce,K. A similar trend may well be at work in SrS:Ce. On the other hand, ion beam analysis revealed that the presence of Na at the interface between the phosphor and insulator may reduce the EL performances [III]. A mobility study indicated that Na diffuses rapidly in SrS:Ce even when annealing is at 600 °C.[32]

efficiency.

Preliminary results showed P and Ga implantation to quench the luminescence of ALE SrS:Ce films.

Since reactively evaporated SrS:Ce,Ag,Mn,Cl has the best reported luminance (170 cd/m^2) among blue-green phosphors, study was made of the possibility of Ag codoping in ALE SrS:Ce thin films by ion implantation. Surprisingly, the implanted SrS:Ce,Ag showed significant PL already after annealing at 500 °C. The PL intensity of samples containing 0.5 at. % Ag and annealed at 800 °C was more than double that of reference samples. Furthermore, decay time at room temperature (RT) had an S_N value of 22 ns, which is the best value recorded for an ALE SrS:Ce based thin film phosphor. Figure 7 shows the plot of S_N values vs emission wavelength of an ALE SrS:Ce and an implanted SrS:Ce,Ag which were annealed at 800 °C, and a reference ALE SrS:Ce which was annealed at 500 °C immediately after deposition. The improved PL properties suggest that codoping with Ag^+ is advantageous in ALE SrS:Ce without the need for other codopants such as used in reactively evaporated SrS:Ce,Ag,Mn,Cl.

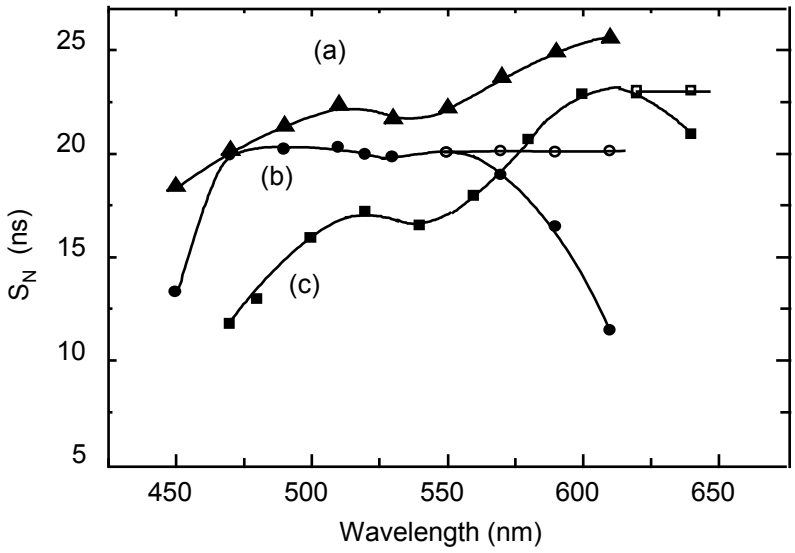

Fig. 7. Comparison of S_N values vs. wavelength for (a) implanted SrS:Ce,Ag (0.5 at.% 800 °C), (b) ALE SrS:Ce (800 °C), and (c) reference ALE SrS:Ce (510 °C). Open squares and circles represent the S_N values after extraction of the fast decay component.

Several test EL devices were fabricated from the implanted SrS:Ce,Ag thin films and studied for their luminance.[33] When driving at 60 Hz, most of the pixels studied in the

neighboring non-implanted area broke down before the turn-on (< 1 cd/m^2), while all the SrS:Ce,Ag pixels exhibited luminance of greater than 10 cd/m^2, despite the samples were treated at 800 °C for 2 hours. Furthermore, the threshold voltage of SrS:Ce,Ag TFEL devices was about 40 V lower than that of the reference ALE SrS:Ce devices. Preliminary studies demonstrate promising results of implanted SrS:Ce,Ag for TFEL applications.

4.2 Implantation of SrS:Cu

The influence of codopants on the luminescence of SrS:Cu was examined by modifying ALE SrS:Cu thin films with Ag, Al, Ga, B, F, and Cl in a dose range of 0.05 to 0.8 at.%.[34] The PL studies were carried out after necessary thermal annealing at temperature of 500 to 800 °C.

In comparison with the reference ALE SrS:Cu, implantation of Ag and Al did not improve the PL intensity, and high doses tended to quench the Cu emission. However, blue emission from Ag centers was observed since, as will be discussed in chapter 5, Ag participates in the luminescence of SrS:Ag,Cu. Interestingly, a number of the implanted SrS:Cu,Ag samples showed only reduced Cu emission.

Implantation of F, Cl, and B improved the PL intensity of SrS:Cu. In particular, implantation of F and especially Cl into green SrS:Cu caused a luminescence shift towards blue. It is not yet clear whether the luminescence of implanted SrS:Cu,Cl is due to emission from the Cu^+ center or to an emission of donor-acceptor pair type after the incorporation of Cl. In the case of implanted SrS:Cu,Ga, the luminescence intensity remained unchanged regardless of the implantation dose. It is worth mentioning that a set of Cu and O co-implanted samples showed codoping of O in SrS:Cu to improve the luminescence intensity.[35]

It is quite possible that the trivalent Ce^{3+} creates Sr vacancy in the SrS host, while monovalent Cu^+ creates S vacancy. Positively charged ions such as K^+ and Ag^+ with right size would be more easily incorporated into SrS:Ce than would negatively charged ions such as F^- and Cl^-; and vice versa, the negative F^- and Cl^- ions might be preferred to the positive Ag^+ and Al^{3+} ions in SrS:Cu. This does not of course exclude the beneficial effects of those less easily

incorporated codopants such as Ag in the case of SrS:Ag,Cu. Nevertheless, ion beam modification of SrS based blue TFEL phosphors has demonstrated the potential of implantation in studying the luminescence properties of dopants and the effects of various codopants. There are a few reports on EL devices prepared by ion implantation,[36] but the modest results have not attracted much attention. However, there seem to be no fundamental reasons why a successful EL device could not be obtained. The full capacity of ion implantation in TFEL applications has yet to be explored.

5. PL and EL of SrS:Cu and SrS:Ag,Cu,Ga

The luminescence of SrS:Cu is known to originate from the isolated Cu^+ ion that substitutes for a Sr atom but locates at an off-center of the octahedral coordination in the host matrix.[37-39] The understanding of the SrS:Cu phosphor has been, however, rather insufficient to interpret many of the luminescence properties. For example, one or more broad bands vary from blue to green in SrS:Cu have been reported in the literature and the explanations were often contradictory.[40-43] Furthermore, the luminescence spectra and decay time of SrS:Cu are strongly temperature dependent but the reasons for this have not been given. On the other hand, most of the alkali halides have the same rock salt crystal structure as SrS, and the luminescence of the octahedrally coordinated Cu^+ in these hosts are well understood,[44-46] they may thus well be used in understanding the luminescence properties of SrS:Cu. The studies carried out in this work were intended to clarify these issues, and possible luminescence mechanisms for SrS:Cu are proposed.

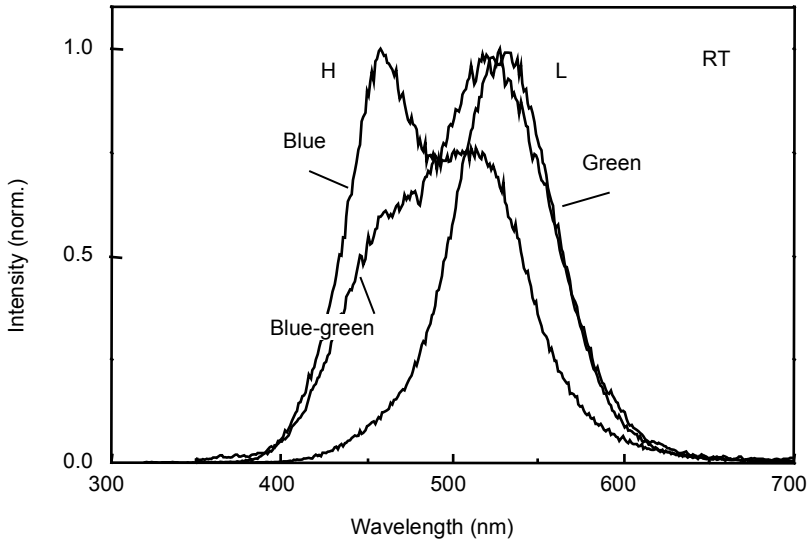

Fig. 8. PL emission spectra of ALE SrS:Cu thin films at RT.

PL studies on ALE SrS:Cu thin films at RT verified that both blue and green luminescence may exist. The emissions of an ALE SrS:Cu consist of a high energy (H) band and a low energy (L) band located at about 460 and 520 nm, respectively (Fig. 8). The ratio of the H and L bands thus determines the color gamut of the phosphor. However, the H band

diminishes as the temperature decreases, as if the emission undergoes a red shift. Completely green luminescent SrS:Cu can be seen as the result of a "single" emission band located at about 530 nm, and this band persists at low temperature. EL of the SrS:Cu films is essentially the same as PL.

The L band is assigned to the isolated Cu^+ ions at an off-center position in the octahedral coordination. Such an assignment is based on the excitation spectrum of SrS:Cu at low temperature, which can be studied only at L band since the H band has vanished. As can be seen from Fig 9, the $^1A_{1g} - {}^3E_g$ peak intensity is much higher than that of $^1A_{1g} - {}^1T_{2g}$. This is a typical off-center characteristic that is well-understood in Cu doped alkali halides.[45] In the case of NaF:Cu^+ where Cu^+ is on-center in the octahedral site, the $^1A_{1g} - {}^1T_{2g}$ peak intensity is significantly enhanced.[46] It needs to be noted that the L band may also contain emission from aggregated Cu centers. Decay studies at the L band at 80 K reveal at least two components. One with the value of 80–110 μs is from the isolated Cu^+ center, while the other 12–18 μs is due to the presence of paired or aggregated Cu^+ centers.

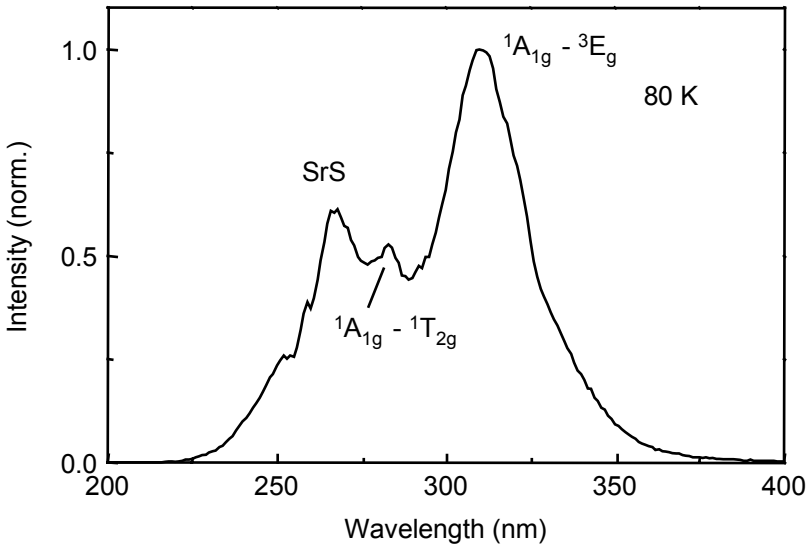

Fig. 9. Excitation spectrum of a SrS:Cu at 80 K.

The H band, which is in large part responsible for the blue emission at high temperature, is due to Cu^+ at a site that experiences different crystal field than the center responsible for the L band. A possible site can be any one of the surrounding eight tetrahedral holes as shown in Fig. 10. The tetrahedral holes have a radius of r_T = 0.77 Å, which makes

them readily available to Cu^+ ion (r_{Cu^+} = 0.77 Å). Also the three nearest S atoms that are shared by the octahedral and the neighboring tetrahedral holes form a relatively open channel (r_c = 0.63 Å), allowing the Cu^+ hop between the holes at high temperature. Furthermore, the weaker ligand-field splitting of the tetrahedral symmetry may cause the lowest excitation state to shift to higher energy as compared with that in an octahedral arrangement.

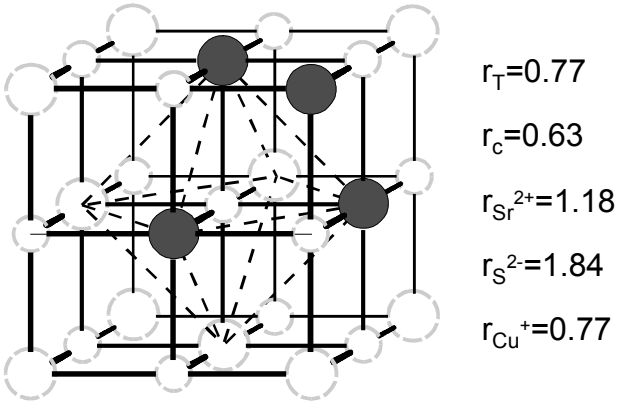

Fig. 10. Unit cell of the SrS structure. A neighboring tetrahedral hole is highlighted.

The large tetrahedral holes may enhance the possibility of forming paired and aggregated Cu centers which may then effectively block the formation of the H band. As a result, "single" green emission is possible. A recent paper reported that alkali metal codoping in MBE SrS:Cu,F results in a red shift of the emission from blue to green.[47] The authors attributed this color shift to reduced Cu coordination number due to the incorporation of alkali metal ions and formation of Cu–S vacancy complexes. The alkali ions together with Cu^+ emission centers were assumed to be acceptors, while S vacancies acted as double donors. However, another likely interpretation is offered here that these alkali ions occupy the tetrahedral holes preventing Cu^+ ions from entering so that results in only green emission.

The temperature dependence of the decay time constant in SrS:Cu leads to a further proposal that, regardless of the two emission bands, the luminescence is likely to follow the three-level mechanism commonly at work in Cu^+ and Ag^+ doped alkali halides.[44,48] Figure 11a illustrates the energy level diagram for this luminescence mechanism. As described in paper [VII], the ^3E_g energy level splits into two sublevels where emissions occur from T_{1g} at low temperature but from T_{2g} at high temperature. Because of the selection rule, the decay is much

longer at T_{1g} (highly populated at low temperature) than at T_{2g} (highly populated at high temperature).

It is worth mentioning that the energies of the two sublevels are very close to each other (~200 cm^{-1}) and cannot correspond to the large energy difference (~2500 cm^{-1}) between the H and L bands in the emission spectra. [VII] In the case of NaF:Cu, a Jahn-Teller effect has been observed as a double-humped band,[46] but such effect is unlikely for SrS:Cu.[39]

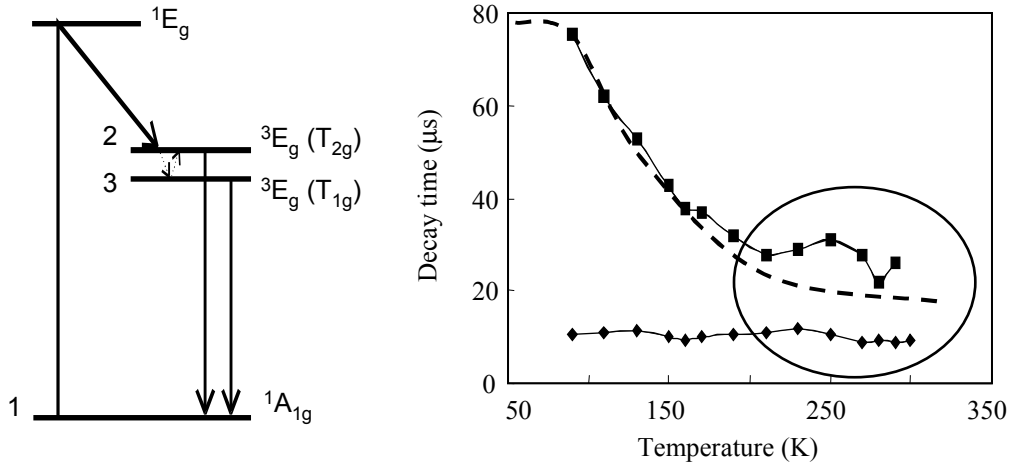

a b

Fig. 11. An illustration of (a) the three-level mechanism, and (b) the fitted decay values as function of temperature.

Some unresolved issues need to be addressed here. As can be seen from Fig. 11b, there are two fitted decay values in a SrS:Cu sample as a function of temperature. Presumably, they are the decay time constants of the isolated (slow component) and paired (fast component) centers. The assumption is nevertheless questionable for the temperature range above 200 K, since the SrS:Cu samples there exhibit extremely long afterglow and the fitted decay values may no longer correspond to the two types of emission centers. Although the decay time constants at temperatures below 80 K were not recorded, it is known that the decay time at 4 K does not differ significantly from that at 80 K.[38] The dotted line shown in Fig. 11b may therefore be a more realistic decay constant vs. temperature curve, which resembles the three-level luminescence.

The assumption that Cu^+ ions locate at tetrahedral sites at high temperature raises another question about the influence of the crystal field on the energy levels of Cu^+ centers and hence the probabilities for electron transition between the excited states and the ground state. A theoretical treatment is desirable to clarify this issue.

The luminescence of SrS:Ag,Cu,Ga films is clearly different from that of SrS:Cu films. As shown in Fig. 12, the EL emission has two broad bands at 80 K, the one located at about 520 nm corresponding to the Cu^+ emission and the new band peaked at 430 nm. These bands coalesce into a single broad band with maximum at 460 nm when samples are at RT. Studies have indicated that the 430 nm peak observed at 80 K is most likely due to the emission of Ag pairs.[49]

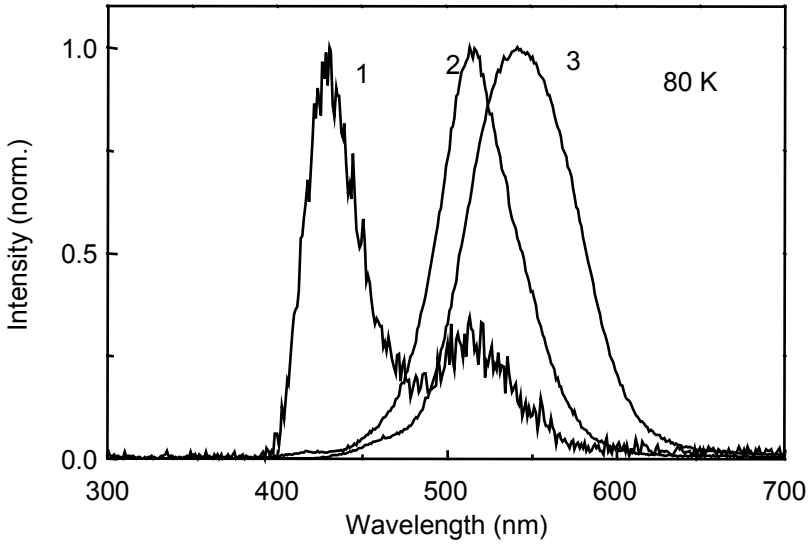

Fig. 12. EL spectra of 1) a SrS:Ag,Cu,Ga, 2) a blue ALE SrS:Cu, and 3) a green ALE SrS:Cu thin films at 80 K.

Two types of luminescence mechanism have been proposed for the SrS:Ag,Cu, Ga phosphor. One suggests that energy transfer takes place from Cu to Ag and results in increased Ag emission.[50] The other, proposed in this work [VII], suggests that the luminescence is a result of the recombination of the excitation energy from Cu^+ and Ag^+ centers at ionized Ag^+–(Ag^+) and Cu^+–(Ag^+) pair centers.

It is probably reasonable to regard these two proposals as pertaining to the same mechanism as is done by Jones et al.[51] Unfortunately, there are no direct experiments to

confirm that this is so. On the other hand, decay studies (Fig. 13) show that the 520 nm emission at 80 K has a very similar decay value to that of SrS:Cu (about 15 and 95 μs), while much faster decay is recorded for the Ag pair emission at 430 nm (9 μs). This indicates that the luminescence events from Ag and Cu activators occur independently, at least at low temperature. More studies on these issues are certainly needed.

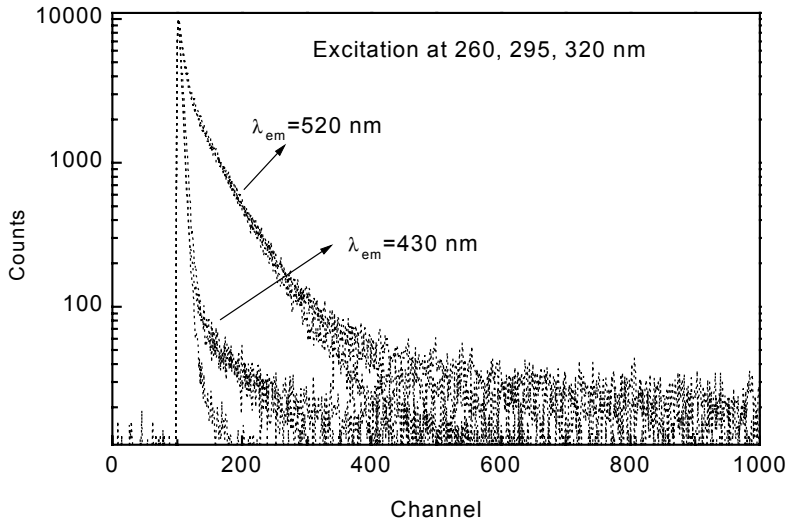

Fig. 13. Decays (at 80 K) of a SrS:Ag,Cu,Ga film studied at 430 and 520 nm emissions with excitations at 265, 295, and 320 nm. Two groups of decay originating from the Ag and Cu centers can be seen regardless of the excitation energy.

6. Conclusions

Combined ion beam analyses reveal that state-of-the-art SrS:Ce thin films made by ALE and reactive evaporation are of high purity. The major impurities are H, C, and O. In the case of ALE SrS:Ce, a good EL performance corresponds to an overall low impurity content, in particular low C content. In intentionally codoped SrS:Ce,Na samples, Na content at the interface clearly reduces the EL performance. Higher content of H, C, and O impurities can be found in reactively evaporated SrS:Ce,Mn,Cl, but the samples outperform ALE SrS:Ce. The results seem to suggest that not only do the overall impurity contents are influential to device performance, but also the location of the impurities may play an important role. For example, impurities at grain boundary may be more tolerable compared with those inside the phosphor crystal. Apparently ion beam analyses are unable to provide such information even though these techniques are powerful in quantifying the impurities and in depth profiling. Attempts to localize the impurities at grains and boundaries were made by using TEM-EDS method. Further studies on the effects of impurities on the EL performance should be conducted in this direction.

Intentional codoping of various ions into ALE SrS:Ce thin films by ion implantation showed that positive ions such as K^+ and Ag^+ are more favorable than negative ions such as F^- and Cl^-, even though codoping with F shifts the emission towards blue without reducing the PL intensity. Implanted SrS:Ce,Ag exhibits excellent PL properties, and the EL results are encouraging. In contrast to SrS:Ce, ion beam modification of ALE SrS:Cu shows that codoping of Ag, Al, or Ga does not improve the PL intensity, whereas incorporation of F, Cl, O, and B does. These findings suggest that there are Sr vacancies in SrS:Ce, but S vacancies dominate in SrS:Cu, so that codopants of opposite charges are favored. Ion implantation has proven to be an efficient way to rapidly examine the effects of codopants in TFEL phosphors. Certainly it can be used to find new EL emitters for a given thin film phosphor host. In contrast to the success of implantation in the semiconductor industry, the performances of ion implanted EL devices have been poor so far. Nevertheless, there would seem to be no fundamental barrier hindering the use of ion implantation for practical EL devices.

PL and EL studies showed that both blue and green emissions exist in SrS:Cu thin films. The color gamut of the phosphor is dependent on the ratio of the two emission bands, i.e. the L and H bands, peaking at 520 and 460 nm, respectively. The L band is attributed to the isolated Cu^+ ion at an off-center position, while the H band may be a Cu^+ center at different site symmetry. The emission is likely to follow a three-level mechanism as characterized by the shortening of decay time with increasing temperature. The completely green luminescence of SrS:Cu with a single band located at about 530 nm may be due to Cu pairs or aggregated Cu centers.

The bright blue luminescence of SrS:Ag,Cu,Ga is associated with Ag centers together with the participation of Cu^+ ions. This is in contrast to the SrS:Ce,Ag phosphor system where the Ag codopant enhances the luminescence of Ce ions but does not participate with its own emission. Current understanding of the luminescence mechanism is limited. A recent study concluded that luminescence is due to the impact ionization at Cu^+ ions where the recombination energy is transferred from Cu^+ to Ag^+. Such an assumption seems to be reasonable though more convincing experiments are needed.

Significant progress has been achieved in finding efficient blue phosphors for full-color TFEL display applications. This has been particularly true during recent years for the SrS based blue EL phosphors. The studies carried out in this work show that the EL performances of state-of-the-art SrS based blue phosphors can be further improved. To improve the phosphor film quality requires, for example reducing the impurity contents in grains, grain boundaries, and phosphor/insulator interfaces, and filling the vacancies (both V_{Sr} and V_S) by one or more suitable codopants. The good properties of SrS:Cu and SrS:Ag,Cu encourage the finding of new paths to the blue phosphors. Recently, renewed studies on CaS:Pb have shown excellent EL results (L_{40}=80 cd/m^2, CIE_x=0.15, CIE_y=0.15, 60 Hz).[52] A priority for the upcoming research will be to improve upon these new results in terms of better stability, luminance and efficiency, and incorporation with phosphors such as ZnS:Mn for achieving full-color. Full-color TFEL displays undoubtedly will be realized in the near future.

Reference

[1] G. Destriau, *J. Chim. Phys.* **34** (1937) 117.

[2] T. Inoguchi, M. Takeda, Y. Kakahara, Y. Nakata, and M. Yoshida, *SID 1974 Digest* **5**, pp. 84.

[3] W.A. Barrow, R.E. Coovert, and C.N. King, *SID 1984 Digest* **15**, pp. 249.

[4] K.O. Velthaus, B. Hüttl, U. Troppenz, R. Hermann, and R.H. Mauch, *SID 1997 Digest* **28**, pp.411.

[5] S.-S. Sun, E. Dickey, J. Kane, and P.N. Yocom, *Conf. Rec. 1997 Inter. Display Res. Conf.*, Toronto, pp. 301.

[6] S.-S. Sun, *4th Inter. Conf. Sci. Tech. Display Phosphors, Extended Abstracts*, Bend, OR, 1998, pp. 183.

[7] S.-S. Sun, *Conf. Rec. 1998 Inter. Display Research Conf., Asia Display'98*, Seoul, CD-ROM.

[8] T. Suntola, in *Handbook of Crystal Growth* **3**, (ed. D.T.J. Hurle), Elsevier, 1994, pp. 605.

[9] E. Soininen, M. Leppänen, and A. Pakkala, *13th Inter. Display Research Conf., Eurodisplay'93*, Strasbourg, 1993, pp. 233.

[10] G. Härkönen, M. Lahonen, E. Soininen, R. Törnqvist, K. Vasama, K. Kukli, L. Niinistö, and E. Nykänen, *4th Inter. Conf. Sci. Tech. Display Phosphors, Extended Abstracts*, Bend, OR, 1998, pp. 223.

[11] B. Hüttl, K.O. Velthaus, U. Troppenz, R. Herrmann, and R.H. Mauch, *J. Cryst. Growth* **159** (1996) 943.

[12] R.H. Mauch, K.O. Velthaus, B. Hüttl, U. Troppenz, and R. Herrmann, *SID 1995 Digest* **26**, pp. 720.

[13] T.A. Oberacker, U. Troppenz, B. Hüttl, T. Gaeryner, R. Herrmann, and K.O. Velthaus, *Conf. Rec. 1997 Inter.Display Res. Conf.*, Toronto, pp. 297.

[14] W. Tong, Y. Xin, M. Chaichimansor, J. Choi, T. Jones, W. Park, B.K. Wagner, C.J. Summers, and S.S. Sun, *4th Inter. Conf. Sci. Tech. Display Phosphors, Extended Abstracts*, Bend, OR, 1998, pp. 339.

[15] H.P. Maruska, T. Parodos, N.M. Kalkhoran, and W.D. Halverson, *Mater. Res. Soc. Symp. Proc.* **345** (1994) 269.

[16] R.T. Holm, S.W. McKnight, E.D. Palik and W. Lukosz, *Appl. Optics* **21** (1982) 2512.

[17] C. Fouassier and A. Garcia, in *Inorganic and Organic Electroluminescence, EL 96 Berlin*, (ed. R.H. Mauch and H.-E. Gumlich), Wissenschaft und Technik, Berlin, 1996, pp. 313.

[18] P. Soininen, E. Nykänen, L. Niinistö, and M. Leskelä, in *Inorganic and Organic Electroluminescence, EL 96 Berlin*, (ed. R.H. Mauch and H.-E. Gumlich), Wissenschaft und Technik, Berlin, 1996, pp. 149.

[19] H. Antson, M. Grasserbauer, M. Hiltunen, T. Koskinen, M. Leskelä, L. Niinistö, G. Stingeder, and M. Tammenmaa, *Fresenius J. Anal. Chem.* **322** (1985) 175.

[20] Unpublished result.

[21] L. Niinistö, *Ann. Chim.* **87** (1997) 221.

[22] T.A. Oberacker and H.W. Schock, *J. Cryst. Growth* **159** (1996) 935.

[23] W. Tong, T. Yang, W. Park, M. Chaichimansour, S. Schön, B.K. Wagner, and C.J. Summers, *J. Electr. Mater.* **26** (1997) 728.

[24] K. Ohmi, T. Hirose, M. Harada, S. Tanaka, and H. Kobayashi, *Jpn. J. Appl. Phys.* **36** (1997) L33.

[25] P. Soininen, L. Niinistö, E. Nykänen, and M. Leskelä, *Appl. Surf. Sci.* **75** (1994) 99.

[26] E. Nykänen, P. Soininen, L. Niinistö, M. Leskelä, and E. Rauhala, in *Proc. 7th Inter. Workshop Electroluminescence*, Beijing, 1994 (Science, Beijing, 1996), pp. 97.

[27] S. Tanda, A. Miyakoshi, and T. Nire, in Electroluminescence, in *Springer Proc. Phys.* **38** (eds. S. Shionoya and H. Kobayashi), Springer-Verlag, Berlin, 1989, pp. 180.

[28] T. Tohda, M. Okajima, M. Yamamoto, and T. Matsuoka, *Jpn. J. Appl. Phys.* **30** (1991) 2786.

[29] U. Troppenz, G. Bilger, W. Bohne, G. Gers, J. Kreissl, R.H. Mauch, K. Sieber, and K.O. Velthaus, in *Inorganic and Organic Electroluminescence, EL 96 Berlin*, (ed. R.H. Mauch and H.-E. Gumlich), Wissenschaft und Technik, Berlin, 1996, pp. 181.

[30] D. Poelman, R. Vercaemst, R.L. Van Meirhaeghe, W.H. Laflere, and F. Cardon, *Jpn. J. Appl. Phys.* **32** (1993) 3477.

[31] B. Hüttle, K. Troppenz, U, Herrmann, and R.H. Mauch, *J. Cryst. Growth* **159** (1996) 943.

[32] R. Lappalainen, M. Karjalainen, R. Serimaa, S. Sevanto, and M. Leskelä, unpublished results.

[33] W.-M. Li, M. Ritala, M. Leskelä, R. Lappalainen, E. Soininen, and L. Niinistö, *5th IUMRS Inter. Conf. Adv. Mater., Abstracts*, 1999, pp. 346.

[34] W.-M. Li, M. Ritala, M. Leskelä, R. Lappalainen, E. Soininen, L. Niinistö, C. Barthou, P. Benalloul, and J. Benoit, *4th Inter. Conf. Sci. Tech. Display Phosphors, Extended Abstracts*, Bend, OR, 1998, pp. 259.

[35] T. Sajavaara, R. Lappalainen, K. Arstila, W.-M. Li, M. Ritala, M. Leskelä, and E. Soininen, *Nucl. Instr. Meth. Phys. Res.* **B 148** (1999) 715.

[36] T. Parodos, H.P. Maruska, W. Halverson, R.A. Budzilek, D. Monarchie, and E. Schlam, *SID 1993 Digest* **24**, pp. 777.

[37] N. Yamashita, *Jpn. J. Appl. Phys.* **30** (1991) 3335.

[38] W. Park, T.C. Jones, W. Tong, B.K. Wagner, C.J. Summers, and S.-S. Sun, *3rd Inter. Conf. Sci. Tech. Display Phosphors, Extended Abstracts*, Huntington Beach, CA, 1997, pp. 57.

[39] T.C. Jones, W. Park, E. Mohammed, B.K. Wagner, C.J. Summers, and S.-S. Sun, in *Flat Panel Display Materials*, (ed. G. Parson, T.S. Fahlen, S. Morozumi, C. Seager, and C.C. Tsai) Materials Research Society, Vol. 508, Pittsburgh, 1998, pp. 281.

[40] W. Lehmann, *J. Electrochem. Soc.* **117** (1970) 1389.

[41] B.B. Laud and V.W. Kulkarni, *J. Phys. Chem. Solids* **39** (1978) 555.

[42] A. Vecht, M. Waite, M.H. Higton, and R. Ellis, *J. Lumin.* **24/25** (1981) 917.

[43] J. Kane, W.E. Harty, M. Ling, and P.N. Yocom, *Conf. Rec. 1985 Inter. Display Res. Conf.,* pp. 163.

[44] B. Moine and C. Pedrini, *Phys. Rev.* **B 30** (1984) 992.

[45] S.A. Payne, *Phys. Rev.* **B 36** (1987) 6125.

[46] D.S. McClure and S.C. Weaver, *J. Phys. Chem. Solids* **52** (1991) 81.

[47] P.D. Keir, J.F. Wager, B.L. Clark, D. Li, and D.A. Keszler, *Appl. Phys. Lett.* **75** (1999) 1398.

[48] C. Pedrini, *Solid State Comm.* **38** (1981) 1237.

[49] U. Troppenz, B. Hüttl, U. Storz, P. Kratzert, and K.-O. Veltaus, *4th Inter. Conf. Sci. Tech. Display Phosphors, Extended Abstracts*, Bend, OR, 1998, pp. 187.

[50] W. Park, T.C. Jones, E. Mohammed, C.J. Summers, and S.S. Sun, *4th Inter. Conf. Sci. Tech. Display Phosphors, Extended Abstracts*, Bend, OR, 1998, pp. 215.

[51] T.C. Jones, W. Park, and C.J. Summers, *Appl. Phys. Lett.* **75** (1999) 2398.

[52] S.J. Yun, Y.S. Kim, J.S. Kang, S.H.K. Park, K.I. Cho, and D.S. Ma, *SID 1999 Digest* **30**, pp. 1142.